Molecular-Weight Distribution Control in Emulsion Polymerization

Antonio Echevarría, José R. Leiza, José C. de la Cal, and José M. Asua
Grupo de Ingeniería Química, Depto. de Química Aplicada, Facultad de Ciencias Químicas, Universidad del País Vasco, 20080 San Sebastián, Spain

Emulsion polymers with well-defined molecular-weight distributions (MWD) were obtained by using a control strategy based on on-line measurements of both unreacted monomer and chain-transfer agent (CTA). The control strategy includes a nonlinear model-based controller that calculates the feed rates of monomer and CTA needed to obtain the desired MWD. This requires a mathematical model for the MWD that was developed based on independent measurements. The control strategy was assessed by computer simulation and experimentally verified by producing polymers with widely different MWDs in the styrene emulsion polymerization using CCl_4 as CTA.

Introduction

Many applications of polymer latexes—adhesives, paper coating, paints, varnishes, and carpet backing—require the formation of a continuous film with high mechanical strength. Both the film-formation process and the mechanical properties of the film depend a great deal on the molecular-weight distribution of the polymer. Thus, latexes including a proper balance of high molecular-weight polymer (which provides adhesive strength and high temperature cleavage) and low molecular-weight polymer (which imparts legginess and compatibility) have been reported to be particularly useful for contact adhesives (Baus and Swift, 1985). Therefore, there is a strong incentive to develop strategies for molecular-weight distribution (MWD) control.

On-line measurement of the MWD would be possible through the use of automated gel permeation chromatography (GPC), but although experimental setups capable of performing this task for solution polymerization have been reported (Ponnuswamy et al., 1988; Budde and Reichert, 1988; Ellis et al., 1988, 1994), to our knowledge no such application has been reported for emulsion polymerization. The lack of hardware sensors might be overcome by software sensors, namely by estimating the MWD from the available on-line measurements of other variables. Although some success has been obtained in solution polymerization systems (Jo and Bankoff, 1976; Schuler and Suzhen, 1985; Schuler and Papadopoulou, 1986; Ellis et al., 1988; Adebekun and Schork, 1989), the compartmentalized nature of emulsion polymerization generally speaking makes the MWD nonobservable from usually available on-line measurements (monomers conversion and temperature). Nevertheless, under some circumstances of practical significance, the MWD of the emulsion polymer is not affected by the compartmentalization of the system. A typical example is when chain-transfer agents (CTA) are used and hence the kinetic length of the growing chain is controlled by the chain-transfer reaction to the CTA instead of by the bimolecular termination. This feature was utilized by Canu et al. (1994) to keep the MWD constant through the polymerization in an open-loop control scheme.

This work is an attempt to obtain emulsion polymers with well-defined MWD by means of a control strategy based on on-line gas-chromatographic measurement of the unreacted monomer and the chain-transfer agent. Several MWDs were considered: (1) polymer with a given average molecular-weight ($\overline{M}_w$) and minimum polydispersity index (PI = 2, because chain growth is controlled by chain-transfer reactions); (2) polymer with arbitrary $\overline{M}_w$ and PI; and (3) polymer with a given bimodal MWD. The unreacted monomer and CTA were determined by gas chromatography by using the experimental setup described elsewhere (Leiza et al., 1993) that is able to deal with high solids content latexes (Urretabizkaia et al., 1994). The instantaneous MWD was estimated through a mathematical model of the process. The mathematical model was used for the off-line calculation of the optimal path to produce the desired polymer in a minimum process time. In order to track this trajectory, a nonlinear model-based controller was used. The control strategy was experimentally ver-

Correspondence concerning this article should be addressed to J. M. Asua.

Table 1. Recipe Used in the Batch-Emulsion Polymerizations (T = 333 K)

Styrene (kg)	0.600
Water (kg)	1.200
SLS (kg)	0.012
KPS (kg)	0.001
$NaHCO_3$ (kg)	0.001
CCl_4(kg)	0; 0.006; 0.012; 0.030; 0.060

ified in the emulsion polymerization of styrene using CCl_4 as CTA.

The organization of the article is as follows: first, the effect of the CTA on the kinetics and the MWD of the emulsion polymerization of styrene is investigated, a mathematical model for the process is developed, and its parameters are fitted using the experimental results. Second, the control strategy is presented. Third, this strategy is assessed by simulation, and finally is experimentally verified.

Kinetics of the Emulsion Polymerization of Styrene Using CCl_4 as Chain-Transfer Agent

The effect of the concentration of CCl_4 (0–10 wt. % based on monomer) on the polymerization rate and on the MWD of the polymer produced in the batch emulsion polymerization of styrene was studied using the recipes given in Table 1. The experimental details are given in Appendix A.

Figure 1 presents the effect of the concentration of CCl_4 on the time evolution of the styrene conversion. It can be seen that the polymerization rate, R_p, decreased as the concentration of CCl_4 increased. In emulsion polymerization, $R_p = k_p[M]_p\bar{n}N_p/N_A$, where k_p is the propagation-rate constant; $[M]_p$ is the concentration of monomer in the polymer particles; $\bar{n}$ is the average number of radicals per particle; N_p is the total number of polymer particles; and N_A is the Avogadro's number. The polymerizations presented in Figure 1 were carried out at the same temperature (k_p = constant) and using a low concentration of CCl_4 (approximately the same

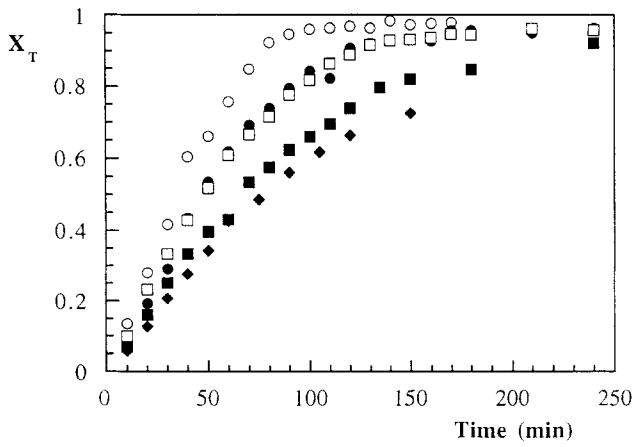

Figure 1. Effect of the concentration of CCl_4 on the evolution of conversion during the styrene emulsion polymerization.

(○) 0% CCl_4; (●) 1% CCl_4; (□) 2% CCl_4; (■) 5% CCl_4; (◆) 10% CCl_4.

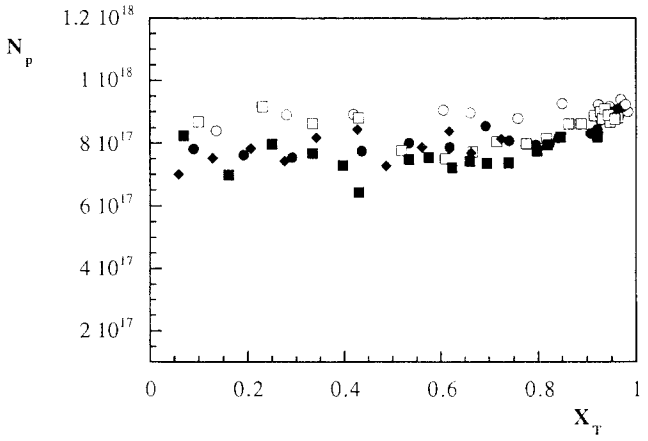

Figure 2. Effect of the concentration of CCl_4 on the evolution of N_p during the styrene emulsion polymerization.

(○) 0% CCl_4; (●) 1% CCl_4; (□) 2% CCl_4; (■) 5% CCl_4; (◆) 10% CCl_4.

$[M]_p$ in all runs). Therefore, the effect of CCl_4 should be on either $\bar{n}$ or N_p. Figure 2 shows the evolution of the total number of polymer particles calculated from the particle-size measurements of the latex samples withdrawn from the reactor. Particle diameters were measured by means of a dynamic light-scattering technique (COULTER N4-PLUS). The experimental error associated with this technique is about 2–8% (depending on the broadness of the particle-size distribution). This leads to errors of about 6–26% in the number of particles. Taking the accuracy of the method into account, Figure 2 shows that N_p was roughly independent of the CCl_4 concentration. This implies that $\bar{n}$ decreases with $[CCl_4]$, probably due to the desorption of the single-unit radicals formed by chain-transfer reaction. It is worth pointing out that the decrease on the polymerization rate when the concentration of CCl_4 was increased was not caused by a reduction of the gel effect due to plastification of the polymer particles by the CCl_4 because, as can be seen in Figure 1, reduction of the polymerization rate occurred even at low conversions (up to 40%) when the concentration of monomer in the polymer particles was about 60% in volume, as there were monomer droplets in the system. Figure 3 presents the evolution of the amount of CCl_4 in the reactor during the polymerizations. It can be seen that only a slight fraction of CCl_4 is consumed during the process. Figure 4 presents the effect of $[CCl_4]$ on the evolution of the number ($\bar{M}_n$) and weight ($\bar{M}_w$) average molecular weight. It can be seen that the greater $[CCl_4]$ the lower the molecular weights. In addition, the molecular weights decreased during the polymerization, probably due to the increase in the ratio $[CCl_4]_p/[M]_p$ because, as shown in Figure 3, the concentration of CCl_4 remained constant during the process, whereas that of styrene decreased. Table 2 shows that cumulative average molecular weight $\bar{M}_n$, calculated at 20% conversion, is inversely proportional to the amount of CCl_4 used in the experiment. Strictly speaking, the cumulative $\bar{M}_n$ can only be equal to the instantaneous $\bar{M}_{ni}$ when conversion approaches zero. However, it can be seen from Figures 3 and 4 that both the amount of unreacted CCl_4 and the average number molecular weight remained

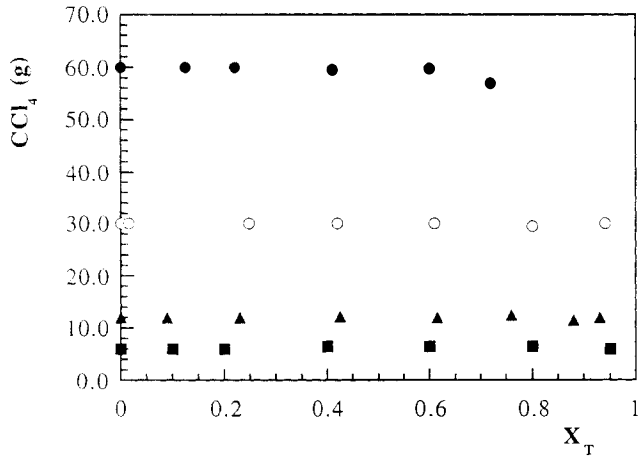

Figure 3. Evolution of the amount of CCl_4 in the reactor.

(■) 1% CCl_4; (▲) 2% CCl_4; (○) 5% CCl_4; (●) 10% CCl_4.

constant up to approximately 50% conversion. Therefore, it is safe to consider that for 20% conversion the cumulative number molecular weight is a good approximation of the instantaneous one.

The fact that $\bar{M}_{ni}$ was inversely proportional to $[CCl_4]$ means that the molecular weight of the polymer was controlled by the chain-transfer reaction. Under these conditions the material balances for the moments of the chain-length distribution of inactive polymer are:

$$\frac{d\nu_k}{dt} = k_f[CCl_4]_p\lambda_k; \qquad k = 0,1, \text{ and } 2, \tag{1}$$

where ν_k and λ_k are the kth-order moment of the chain-length distribution of inactive and active chains, respectively; and k_f is the rate coefficient for the chain-transfer reaction. Note that the material balance applies to the whole reactor content. Assuming that the pseudo-steady-state conditions apply for the active chains, the moments of the chain-length distribution of these chains can be readily obtained from the balances of active chains, considering the chain-transfer reaction as the sole termination mechanism:

$$\lambda_0 = \bar{n}N_p \tag{2}$$

$$\lambda_1 = \frac{k_p[M]_p}{k_f[CCl_4]_p}\lambda_0 \tag{3}$$

$$\lambda_2 = \frac{2\lambda_1^2}{\lambda_0}. \tag{4}$$

Notice that ν_k is a cumulative property, whereas λ_k is an instantaneous one.

The cumulative average molecular weights are

$$\bar{M}_n = \frac{\nu_1}{\nu_0}P_m = \bar{X}_nP_m \tag{5}$$

$$\bar{M}_w = \frac{\nu_2}{\nu_1}P_m = \bar{X}_wP_m, \tag{6}$$

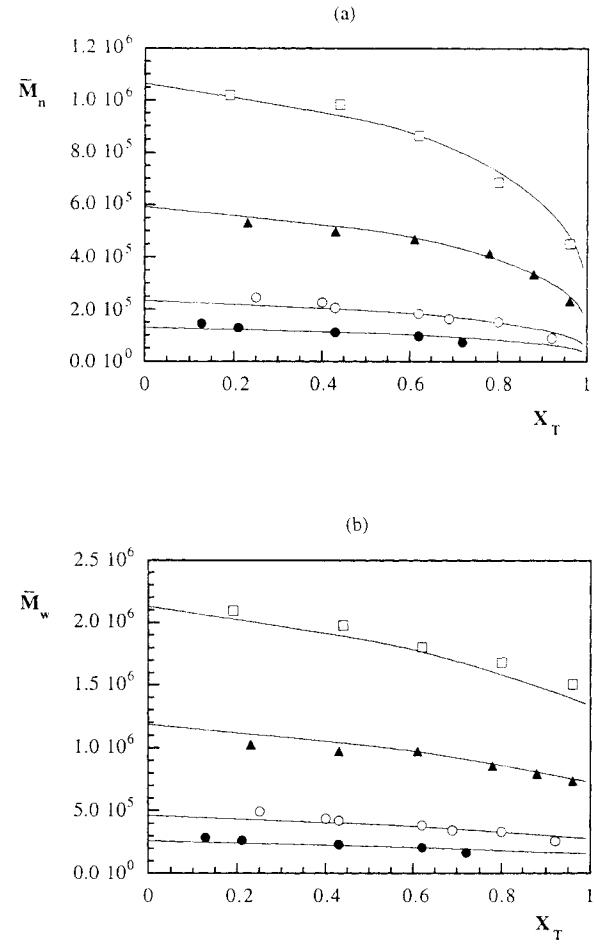

Figure 4. Effect of $[CCl_4]$ on the evolution of (a) $\bar{M}_n$ and (b) $\bar{M}_w$.

(□) 1% CCl_4; (▲) 2% CCl_4; (○) 5% CCl_4; (●) 10% CCl_4; (—) model predictions.

where $\bar{X}_n$ and $\bar{X}_w$ are the cumulative number and weight average lengths, respectively, and P_m is the molecular weight of the monomer. The instantaneous values of the number and weight average chain lengths are:

$$\bar{X}_{ni} = \frac{d\nu_1/dt}{d\nu_0/dt} = \frac{k_p[M]_p}{k_f[CCl_4]_p} \tag{7}$$

$$\bar{X}_{wi} = \frac{d\nu_2/dt}{d\nu_1/dt} = 2\frac{k_p[M]_p}{k_f[CCl_4]_p}. \tag{8}$$

From these values the instantaneous molecular-weight distribution can be calculated by using the Schulz-Flory distribution (Billmeyer, 1962):

Table 2. $\bar{M}_n$ Values at $X_T = 0.2$

CCl_4	1%	2%	5%	10%
$\bar{M}_n$	1×10^6	5×10^5	2×10^5	1×10^5

$$W(n) = \frac{y(ny)^z \exp[-ny]}{\Gamma(z+1)} \tag{9}$$

$$z = \frac{1}{\frac{\overline{X}_{wi}}{\overline{X}_{ni}} - 1} \tag{10}$$

$$y = \frac{z+1}{\overline{X}_{wi}}, \tag{11}$$

where $W(n)$ is the weight fraction of chains of length n, and Γ is the gamma function. When the termination is controlled by transfer to the CTA reaction, $\overline{X}_{wi}/\overline{X}_{ni} = 2$ and Eq. 9 reduces to

$$W(n) = \frac{n}{\overline{X}_{ni}^2} \exp\left[-\frac{n}{\overline{X}_{ni}}\right]. \tag{12}$$

The cumulative molecular-weight distribution, $W_c(n)$, can be calculated as follows:

$$W_c(n) = \frac{1}{X_T} \int_0^{X_T} W(n)\, dX_T, \tag{13}$$

where X_T is the monomer conversion given by

$$\frac{dX_T}{dt} = \frac{k_p}{M_0} [M]_p \bar{n} \frac{N_p}{N_A}, \tag{14}$$

where M_0 is the number of moles of monomer in the recipe.

To integrate the model it is more convenient to use the differential form of Eq. 13:

$$\frac{dW_c(n)}{dt} = \frac{1}{X_T} [W(n) - W_c(n)] \frac{dX_T}{dt}. \tag{15}$$

The goal of this part of the work is to obtain a mathematical model for the MWD that can be used for control purposes. The model, as written in Eqs. 1 to 15, has as independent variable, the time, and the time evolution of the MWD depends on $\bar{n} \times N_p$. Unfortunately, there is no way to accurately predict this value, although the problem can be overcome by using conversion as the independent variable. This can be achieved by dividing Eqs. 1 and 15 by Eq. 14:

$$\frac{d\nu_o}{dX_T} = M_0 N_A \frac{k_f[CCl_4]_p}{k_p[M]_p} \tag{16}$$

$$\frac{d\nu_1}{dX_T} = M_0 N_A \tag{17}$$

$$\frac{d\nu_2}{dX_T} = 2M_0 N_A \frac{k_p[M]_p}{k_f[CCl_4]_p} \tag{18}$$

$$\frac{dW_c(n)}{dX_T} = \frac{1}{X_T} [W(n) - W_c(n)]. \tag{19}$$

The partitioning of the monomer and CTA between the different phases can be calculated by means of the overall material balances and the following equilibrium equations (Gugliotta et al., 1995; Armitage et al., 1994; and Echevarría et al., 1995):

$$\frac{[i]_p}{[i]_w} = K^i_{p,w} \tag{20}$$

$$\frac{[i]_d}{[i]_w} = K^i_{d,w} \tag{21}$$

where $i = M$ and CCl_4, p represents the polymer particles, w the aqueous phase, and d the monomer droplets.

The parameters of the model taken from literature are given in Table 3. The values of k_f, $K^{CCl_4}_{p,w}$, and $K^{CCl_4}_{d,w}$ were estimated by means of the Nelder and Mead approach (Nelder and Mead, 1964), minimizing the following objective function:

$$J = \sum_{i=1}^{m} \sum_{j=1}^{n(i)} \left[\left(\overline{M}_{n_{\text{exp}}} - \overline{M}_{n_{\text{theor}}} \right)^2_{i,j} + \left(\overline{M}_{w_{\text{exp}}} - \overline{M}_{w_{\text{theor}}} \right)^2_{i,j} \right], \tag{22}$$

where m is the number of experiments, $n(i)$ the number of measurements in the experiment i, and the subscripts exp and theor refer to the experimental and theoretical values, respectively.

The estimated values of the parameters are presented in Table 3. Figure 4 presents a comparison between the experimental values and the model predictions of $\overline{M}_n$ and $\overline{M}_w$. It can be seen that a fairly good agreement was achieved. A more exigent test is to compare the evolution of the MWD experimentally determined by GPC with that predicted by the model. The MWD obtained from the GPC measurements and that given by Eq. 19 use a different normalization. The GPC distribution is usually normalized to one, and log (D) is used in the X-axis, being $D = nP_m$. The GPC distribution is written as

$$W_{\text{GPC}}(D) = \frac{df}{d(\log D)}, \tag{23}$$

where f is the weight fraction.

On the other hand, the theoretical development of the molecular-weight distribution is also normalized to one, but n (chain length) is used in the X-axis as follows:

Table 3. Values of the Parameters of the Model

k_p*	k_f**	(m³/mol·s)	0.275	2.695×10^{-3}
$K^{M\dagger}_{p,w}$	$K^{M\dagger}_{d,w}$		1,500	2,700
$K^{CCl_4**}_{p,w}$	$K^{CCl_4**}_{d,w}$		3,650	4,860
$\rho^{\ddagger}_M$	$\rho^{\ddagger}_{CCl4}$	kg/m³	904	1,590
$\rho^{\ddagger}_{\text{pol}}$		kg/m³	1,050	

*Buback et al. (1988).
**Estimated value.
†Gardon (1968).
‡Brandup and Immergut (1989).

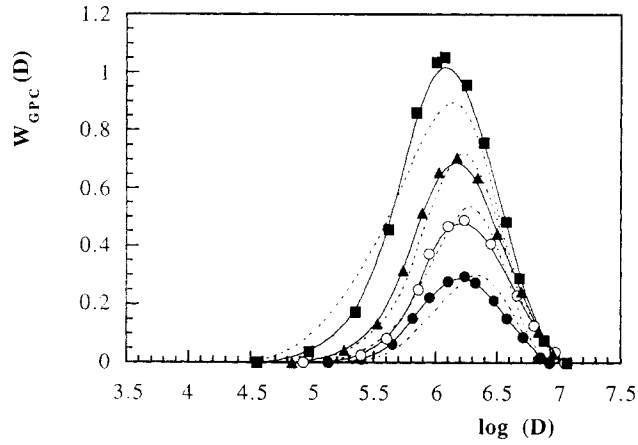

Figure 5. Comparison between the experimental and model-predicted MWDs during the emulsion polymerization of styrene with 1% of CCl_4 at different conversions.

(---) model predictions; experimental (-●-) $X_T = 0.19$; (-○-) $X_T = 0.43$; (-▲-) $X_T = 0.62$; (-■-) $X_T = 0.96$.

$$W_c(n) = \frac{df}{dn}. \tag{24}$$

Combining Eqs. 23 and 24, the following relationship between the GPC distribution and that calculated by Eq. 19 is easily obtained

$$W_{GPC}(D) = W_c(n) n \ln(10). \tag{25}$$

Figures 5 to 8 present a comparison between the MWDs determined experimentally and those calculated by the model using the parameters in Table 3. It can be seen that a very good agreement was obtained.

Once a mathematical model for the MWD was available, on-line control of the MWD was attempted.

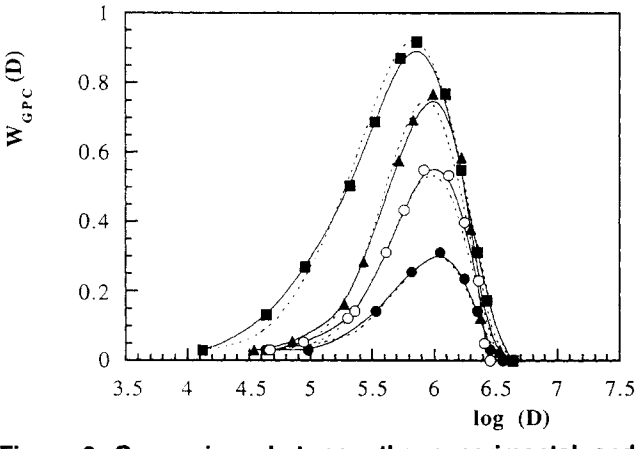

Figure 6. Comparison between the experimental and model-predicted MWDs during the emulsion polymerization of styrene with 2% of CCl_4 at different conversions.

(---) model predictions; experimental (-●-) $X_T = 0.23$; (-○-) $X_T = 0.43$; (-▲-) $X_T = 0.61$; (-■-) $X_T = 0.96$.

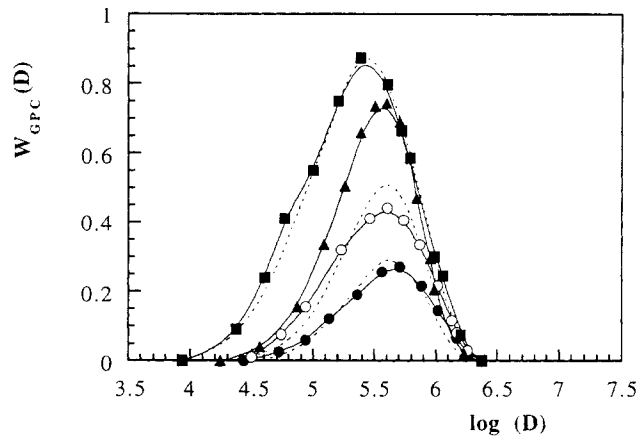

Figure 7. Comparison between the experimental and model-predicted MWDs during the emulsion polymerization of styrene with 5% of CCl_4 at different conversions.

(---) model predictions; experimental (-●-) $X_T = 0.25$; (-○-) $X_T = 0.43$; (-▲-) $X_T = 0.62$; (-■-) $X_T = 0.92$.

Control Strategy

The goal of this work is to obtain emulsion polymers with well-defined MWD by using a control strategy based on on-line measurements of the unreacted monomer and CTA. Figure 9 summarizes the control scheme. Note that the proposed control technique can only be implemented when the chain stoppage is mainly by transfer to CTA. Samples are withdrawn from the reactor using the experimental setup developed by Leiza et al. (1993), and the unreacted monomer and CTA measured by on-line gas chromatography. In order to estimate the amounts of monomer and CTA in the polymer particles from these experimental results, a state-estimation technique based on nonlinear optimization (Jang et al., 1986) was used. This algorithm allows the estimation of $[M]_p$, $[CCl_4]_p$, and $\bar{n} \times N_p$. These values are then used to update the estimated states to compensate for the delay due to sam-

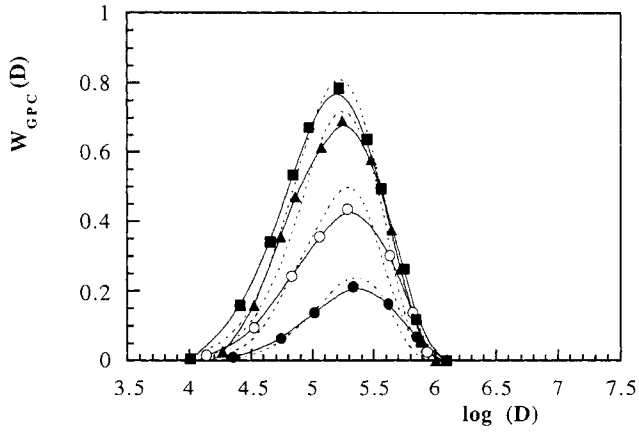

Figure 8. Comparison between the experimental and model-predicted MWDs during the emulsion polymerization of styrene with 10% of CCl_4 at different conversions.

(---) model predictions; experimental (-●-) $X_T = 0.21$; (-○-) $X_T = 0.43$; (-▲-) $X_T = 0.62$; (-■-) $X_T = 0.72$.

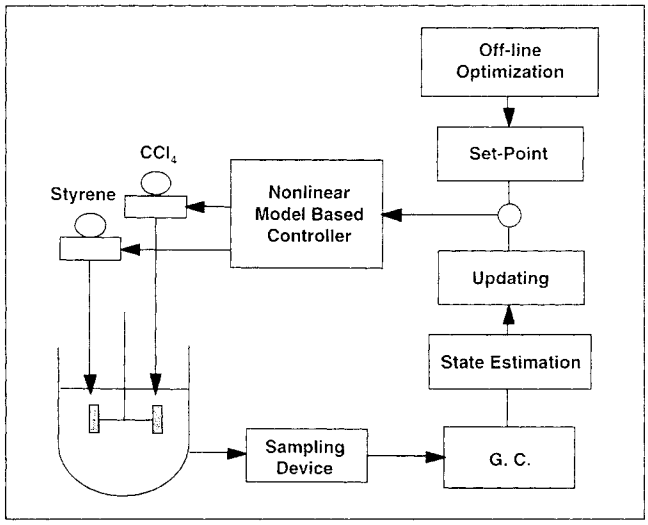

Figure 9. Control scheme.

pling, gas chromatographic (GC) analysis, and computer calculation. The updated values are compared with the set point calculated by means of an off-line optimization, and then a nonlinear model-based controller was used to calculate the control actions for the next time interval. The different parts of the control strategy are explained below.

Optimization algorithm

The goal of the optimization algorithm is to calculate the set point trajectories of the controlled variables that ensure the production of an emulsion polymer of the desired MWD in a minimum process time. The process time was chosen as the objective function and the polymer quality (MWD) was one of the constraints. The objective function was obtained from the monomer material balance,

$$\frac{dX_T}{dt} = Rp; \qquad t_{\text{fin}} = \int_0^1 \frac{1}{R_p} dX_T, \tag{26}$$

and hence the objective function to be minimized is

$$\underset{[M]_p}{\text{Min}} \left[\int_0^1 \frac{1}{R_p} dX_T \right] \tag{27}$$

where R_p is the polymerization rate, X_T is the overall conversion defined as the ratio between the polymer in the reactor and the monomer in the recipe, and t_{fin} is the final process time.

In the optimization, it was assumed that R_p increased with $[M]_p$. This might not be the case if a strong gel effect occurs, but Figure 1 does not present evidence of this effect (increase of the slope as conversion increases). On the other hand, the instantaneous number average molecular weight is a function of the ratio of the concentrations of monomer and CTA in the polymer particles (see Eq. 7), and hence to produce a desired molecular weight, the higher the $[M]_p$, the higher the $[\text{CTA}]_p$. Note that this ratio can be obtained by using large or small values of $[M]_p$ and $[\text{CTA}]_p$. If we wish to produce a desired molecular weight and to work at the maximum polymerization rate, the dependence of $\bar{n} \times N_p$ on the concentration of CCl_4 must be taken into account. In this work this relationship was experimentally calculated as $\bar{n} \div [CCl_4]^{-0.23}$. Therefore, the polymerization rate can be written as follows:

$$R_p \div \frac{[M]_p}{[CCl_4]^{0.23}}. \tag{28}$$

On the other hand, $[M]_p/[CCl_4]_p$ is fixed for a given molecular weight. Therefore the following relationship holds:

$$[CCl_4] \div [M]_p. \tag{29}$$

Combining Eqs. 28 and 29, one gets

$$R_p \div [M]_p^{0.77}. \tag{30}$$

This means that in order to maximize the polymerization rate, it is necessary to work at each time at the maximum concentration of monomer in the particles.

The minimization of Eq. 27 is subject to the following constraints:

1. The polymer produced must have the desired final MWD $[W_c^d(n)]$. It is convenient to reformulate this constraint in terms of the instantaneous MWD that has to be produced at each value of X_T.

$$\bar{X}_{ni} = f(X_T). \tag{31}$$

Note that the MWD for this particular case is defined by the instantaneous number average molecular weight, $\bar{X}_{ni}$. Therefore, to produce a given final $W_c^d(n)$, it is sufficient to produce the required $\bar{X}_{ni}$ at each conversion interval. The method used in this work to obtain Eq. 31 is presented in Appendix B.

2. The maximum amounts of monomer and chain transfer agent that can be in the reactor are the total amount in the recipes $M_{\max}$ and $CCl_{4_{\max}}$.

$$M_f + M_{\text{pol}} \le M_{\max} \tag{32}$$

$$CCl_{4_f} + CCl_{4_{\text{pol}}} \le CCl_{4_{\max}}, \tag{33}$$

where the subscripts f and pol stand for free and polymerized amounts, respectively.

The value of $M_{\max}$ is given by the solids content of the formulation and the volume of the reactor. The value of $CCl_{4_{\max}}$ depends on the trade-off between the process time and the amount of offspec polymer. As the CTA accumulates in the reactor, for a given amount of CTA there is a critical overall conversion, X_T^*, from which only molecular weights lower than the desired ones can be obtained. This critical conversion can be increased by decreasing the amount of CTA, but this leads to a decrease of $[M]_p$, and consequently to an increase in the process time. In this work, the critical overall conversion has been set equal to 0.95, namely, 5% of the offspec polymer was allowed. Given X_T^*, the values of $\bar{X}_n$

and $\bar{X}_{ni}$ can be obtained from the minimization of Eq. B-2 (Appendix B). These values are related with the amounts of free and polymerized monomer and CTA as follows:

$$\bar{X}_n = \frac{M_{\text{pol}}}{\text{CCl}_{4\text{pol}}} \tag{34}$$

$$\bar{X}_{ni} = \frac{k_p[M]_p}{k_f[\text{CCl}_4]_p} \cong \frac{k_p M_f}{k_f \text{CCl}_{4_f}} \tag{35}$$

$$M_f = M_{\max}(1 - X_T^*). \tag{36}$$

Equations 34–36 allow the calculation of CCl_{4f} and $\text{CCl}_{4\text{pol}}$, and hence the value of $\text{CCl}_{4\max}$.

3. The monomer and CTA already charged into the reactor cannot be removed:

$$\frac{d[M_f + M_{\text{pol}}]}{dX_T} \geq 0 \tag{37}$$

$$\frac{d[\text{CCl}_{4f} + \text{CCl}_{4\text{pol}}]}{dX_T} \geq 0. \tag{38}$$

4. The amount of monomer and hence that of CCl_4 in the latex particles should be limited. The presence of droplets should not be allowed, as the excess of monomer or CCl_4, which is in the monomer droplets, does not contribute to increasing the polymerization rate, but causes a significant loss of control capacity. Safety may also be a reason to limit the amount of free monomer in the reactor. Following Echevarría et al. (1995), the maximum concentrations of the monomer and CCl_4 in the latex particles used in this work were those corresponding to the saturation of polymer particles.

The optimization provides the amounts of both monomer and CTA in the reactor at any X_T. This result is independent of the polymerization rate of the process and can be regarded as master curves. Figure 10a presents an example of these curves for the desired MWD of Figure 10b.

State estimation

A mathematical model of the process was used to fit the amounts of free monomer and CTA measured on-line by gas chromatography, being the evolution of the adjustable parameter $\bar{n} \times N_p$ (Urretabizkaia et al., 1994). The following objective function was minimized:

$$J = \sum_{i=m-2}^{m} \sum_{i=M,\text{CCl}_4} [i_{\text{exp}}(t) - i_{\text{cal}}(t)]^2, \tag{39}$$

where m is the last sample available, i_{exp} is the amount of i measured by on-line GC, and i_{cal} is the value calculated with the model. Note that the last three experimental data were used in the objective function. The values of i_{cal} were calculated by means of the following equations:

$$\frac{dM}{dt} = -k_p[M]_p \frac{\bar{n}N_p}{N_A} + F_M \tag{40}$$

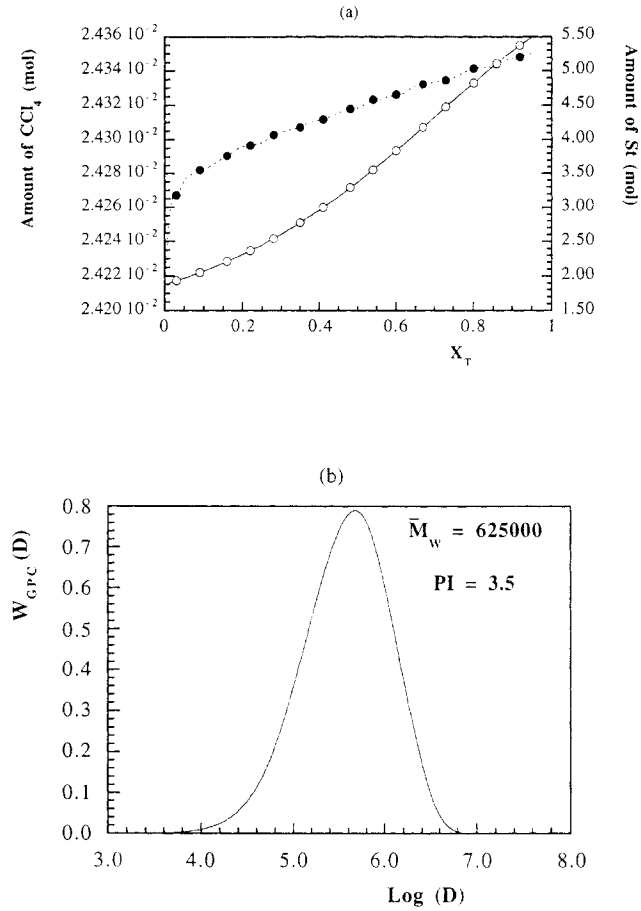

Figure 10. Amounts of monomer (---●---) and CTA (-○-) to be added to the reactor at any X_T (a) to obtain the MWD in part (b).

$$\frac{d\text{CCl}_4}{dt} = -k_f[\text{CCl}_4]_p \frac{\bar{n}N_p}{N_A} + F_{\text{CCl}_4} \tag{41}$$

where F_M and F_{CCl_4} are the molar feed flow rates of the monomer and CTA, respectively.

The product $\bar{n} \times N_p$ was used as an adjustable parameter. For this purpose, $\bar{n} \times N_p$ was approximated by the following equation:

$$\bar{n} \times N_p = k_1 + k_2 t, \tag{42}$$

and the parameters k_1 and k_2 were tuned to minimize Eq. 39 by means of an algorithm for parameter estimation in ordinary differential equations (Seinfeld and Lapidus, 1974). Once the parameters of Eq. 42 are estimated, the predictions of the mathematical model are used as estimations of the free monomer, $\hat{M}$, and CTA, $\hat{\text{CCl}}_4$, in the reactor, as well as those of their concentrations in the polymer particles, $[\hat{M}]_p$ and $[\hat{\text{CCl}}_4]_p$.

Updating of the state estimates

For this system there is a time delay of 8 min (2.5 min for sample preparation, 4 min for GC analysis, and 1.5 min for

calculations), that is, the estimated values of the state variables correspond to the situation of the reactor at the sampling time. Therefore, the state estimates must be updated. This is done by integrating Eqs. 40 and 41 from the sampling time to the current time. The time dependence of $\bar{n} \times N_p$ given by Eq. 42 was used in the integration.

Nonlinear model-based controller

The role of the nonlinear model-based controller is to calculate the feed rates of monomer and CTA until the next measurement is available, that is, for the next 8 min. The controller is based on the discretization of the material balances:

$$M_{n+1} = \hat{M}_n + \left(F_M - k_p [M]_p \frac{\bar{n} N_p}{N_A} \right) \Delta t \tag{43}$$

$$\mathrm{CCl}_{4_{n+1}} = \hat{\mathrm{CCl}}_{4_n} + \left(F_{\mathrm{CCl}_4} - k_f [\mathrm{CCl}_4]_p \frac{\bar{n} N_p}{N_A} \right) \Delta t, \tag{44}$$

where $\hat{i}_n$ are the updated values of monomer and CTA at the beginning of the control interval Δt, i_{n+1} are the desired values of these variables at the end of the interval, and $\bar{n} \times N_p$ is given by Eq. 42. The values of i_{n+1} are given by the master curves obtained by means of the off-line optimization and depend on the overall conversion:

$$i_{n+1} = f(X_{T_{n+1}}) \tag{45}$$

$$X_{T_{n+1}} = \frac{M_0 + \int_0^{t_{n+1}} F_M \, dt - M_{n+1}}{M_{\max}}. \tag{46}$$

The iterative solution of Eqs. 43–46 yields the values of F_M and F_{CCl_4} for the next time interval.

The time delay and the fact that at least two on-line measurements are required to estimate the time evolution of $\bar{n} \times N_p$ means that no control action could be implemented for a process interval of 16 min. If the polymerization were conducted under the conditions calculated in the optimization, that is, at a high polymerization rate, a significant fraction of the polymer would be formed in an open-loop control mode, which does not guarantee the formation of the desired polymer. In order to minimize this risk, the first 16 min of the reactions were carried out in an open-loop control mode, but with a low concentration of monomer and CTA in the reactor. In this way, only a limited amount of polymer was produced. Once the estimation of $\bar{n} \times N_p$ was available, the feed flow rates were calculated as explained earlier.

Assessing the Control Strategy by Numerical Simulation

The control strategy was first assessed by numerical simulation. Three cases were considered:

S1: Polymer of $\bar{M}_w = 400{,}000$ and PI = 2 (minimum possible value).

S2: Polymer of $\bar{M}_w = 625{,}000$ and PI = 3.5 (broad distribution).

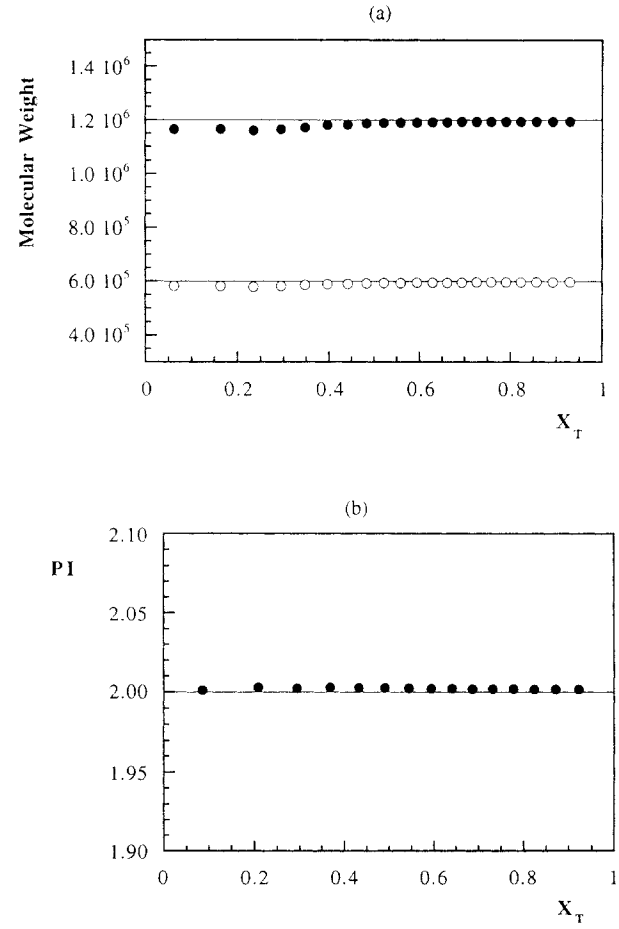

Figure 11. Evolution of (a) $\bar{M}_n$, $\bar{M}_w$ and (b) PI for case S1.

(a) (—) desired; (●) simulated $\bar{M}_w$; (○) simulated $\bar{M}_n$; (b) (—) desired; (●) simulated PI.

S3: Polymer with bimodal MWD: $\bar{M}_{w1} = 10^6$; $\mathrm{PI}_1 = 2$; $\bar{M}_{w2} = 10^5$; $\mathrm{PI}_2 = 2$.

A detailed mathematical model was used to simulate the process. To make the outputs of the model closer in character to the real data, a 2% random error was added to the amounts of unreacted monomer and CTA calculated by the model for $X_T > 0.2$. For $X_T < 0.2$, a larger random error (5%) was used to account for the effect of the presence of monomer droplets on the GC measurements. The measurements were assumed to be delayed by 8 min, and the first 16 min of the polymerization were carried out in an open-loop mode. Figures 11–13 present a comparison between the evolution of the desired and simulated $\bar{M}_n$, $\bar{M}_w$, and PI for the three cases considered. It can be seen that fairly good agreement was achieved, the slight deviation observed at low conversions being due to the errors associated with the open-loop control used in this part of the polymerizations.

Experimental Validation of the Control Strategy

The control strategy was experimentally validated for the unseeded emulsion polymerization of styrene using CCl_4 as CTA. The materials used are described in Appendix A. Polymerizations were carried out in the equipment developed by

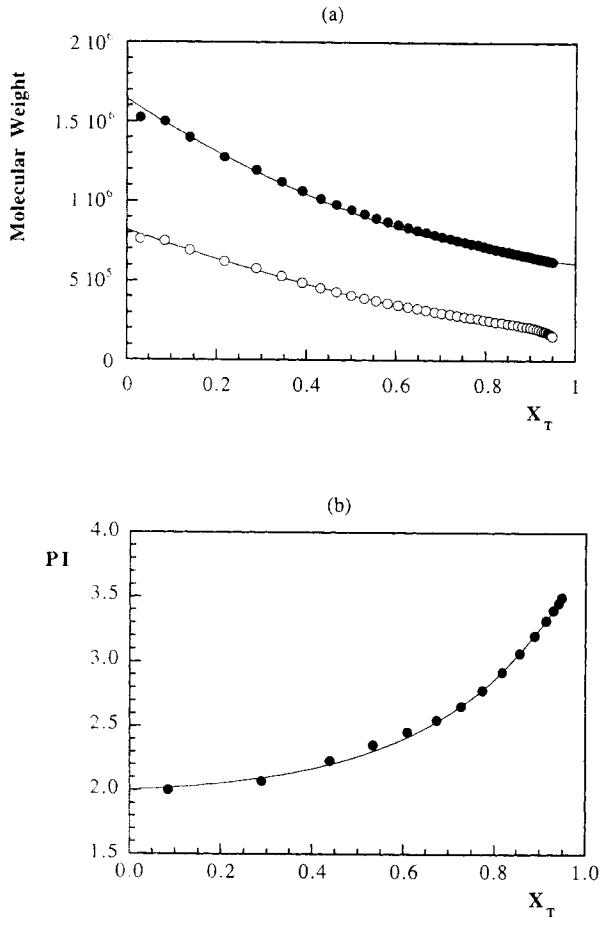

Figure 12. Evolution of (a) $\overline{M}_n$, $\overline{M}_w$ and (b) PI for case S2.

(a) (—) desired; (●) simulated $\overline{M}_w$; (○) simulated $\overline{M}_n$; (b) (—) desired; (●) simulated PI.

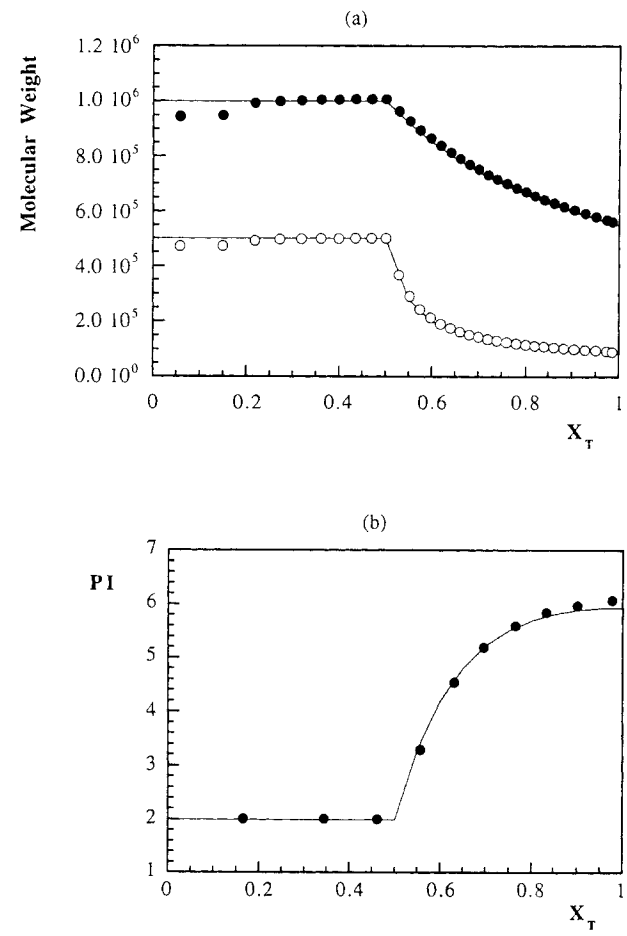

Figure 13. Evolution of (a) $\overline{M}_n$, $\overline{M}_w$ and (b) PI for case S3.

(a) (—) desired; (●) simulated $\overline{M}_w$; (○) simulated $\overline{M}_n$; (b) (—) desired; (●) simulated PI.

Leiza et al. (1993). Samples were also taken for the off-line measurement of the MWD (by GPC) and monomer conversion (by gravimetry). Three cases were considered:

C1: Polymer of minimum PI.

C1a: $\overline{M}_w = 400{,}000$; $\overline{M}_n = 200{,}000$ (PI = 2).

C1b: $\overline{M}_w = 1{,}200{,}000$; $\overline{M}_n = 600{,}000$ (PI = 2).

C2: Polymer of $\overline{M}_w = 625{,}000$ and PI = 3.5.

C3: Polymer with bimodal MWD: $\overline{M}_{w1} = 10^6$; $PI_1 = 2$; $\overline{M}_{w2} = 10^5$; $PI_2 = 2$.

Case C1. The optimization shows that all the CTA should be included in the initial charge and the process controlled by the feed rate of styrene. Table 4 presents the recipes used in these polymerizations. In this case, the MWD has to be kept constant during the process. Figure 14 presents the evolution of the off-line-measured $\overline{M}_w$ and $\overline{M}_n$ for cases C1a and C1b. The comparison of the whole MWD for cases C1a and C1b is presented in Figures 15 and 16, respectively. It can be seen that a polymer of the desired quality was obtained.

Case C2. The desired MWD was discretized in 20 instantaneous MWDs, as explained in Appendix B. In the optimization, it was calculated that about 30% of the total styrene should be included in the initial charge. Due to the time required to make the first control action (16 min), such a big charge may result in a substantial fraction of offspec polymer. Therefore, a smaller initial charge was used and for the first 16 min arbitrarily fixed small feed rates of styrene and CCl_4 were used. Once a good estimation of $\bar{n} \times N_p$ was available, the control actions calculated by the nonlinear model-based controller were implemented. Table 5 presents the

Table 4. Recipes used in case C1

kg	Total	Initial charge	Feed
	C1a		
St	0.600	0.050	0.550
H_2O	1.200	0.800	0.400
CCl_4	0.0027	0.0027	0
$K_2S_2O_8$	0.001	0.001	0
$NaHCO_3$	0.001	0.001	0
SLS	0.012	0.007	0.005
	C1b		
St	0.600	0.049	0.551
H_2O	1.200	0.800	0.400
CCl_4	0.0009	0.0009	0
$K_2S_2O_8$	0.001	0.001	0
$NaHCO_3$	0.001	0.001	0
SLS	0.012	0.007	0.005

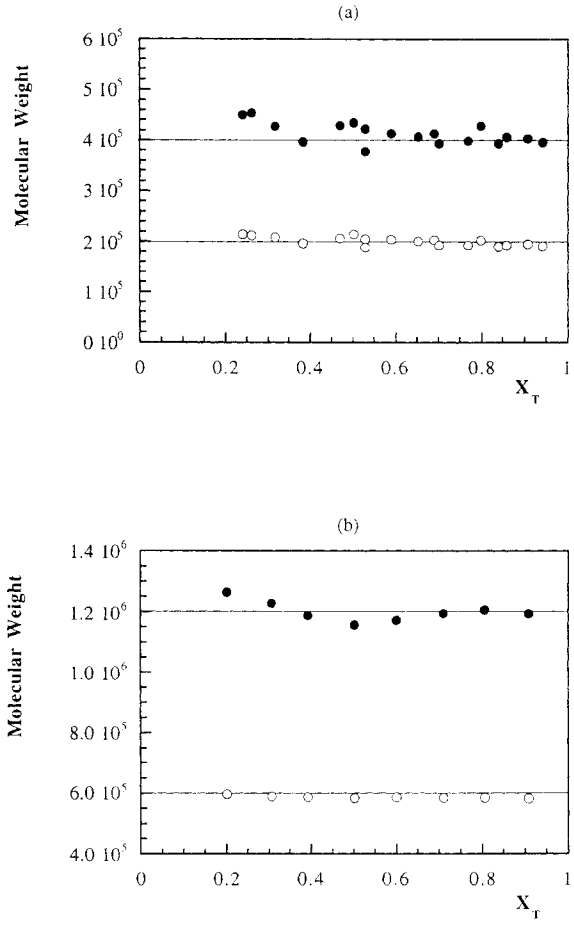

Figure 14. Evolution of $\bar{M}_w$ and $\bar{M}_n$ for cases (a) C1a and (b) C1b.

(—) desired; (●) experimental $\bar{M}_w$; (○) experimental $\bar{M}_n$.

recipe used in this polymerization. Figure 17 presents the evolution of $\bar{M}_w$ and $\bar{M}_n$ measured off-line by GPC and that of the desired polymer. Figure 18 presents the evolution of the MWD during this process. It can be seen that the control strategy was successfully applied to produce a polymer of the

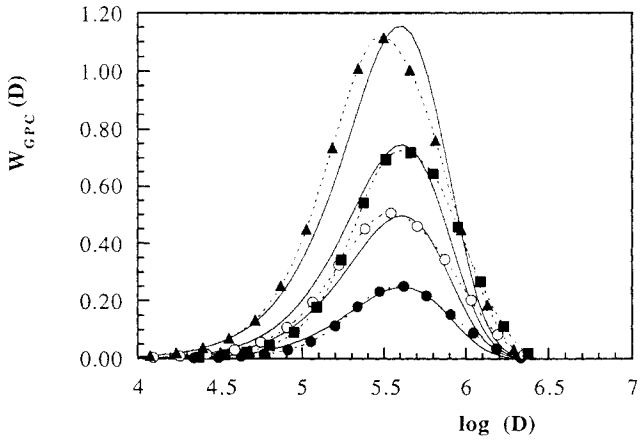

Figure 15. Evolution of the MWD for case C1a.

(—) desired; experimental (--●--) $X_T = 0.24$, (--○--) $X_T = 0.38$, (--■--) $X_T = 0.59$, (--▲--) $X_T = 0.94$.

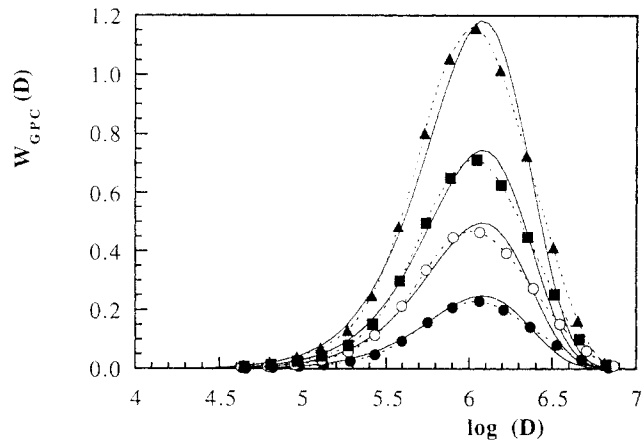

Figure 16. Evolution of the MWD for case C1b.

(—) desired; experimental (--●--) $X_T = 0.24$, (--○--) $X_T = 0.38$, (--■--) $X_T = 0.59$, (--▲--) $X_T = 0.94$.

Table 5. Recipes Used in Case C2

kg	Total	Initial Charge	Feed
St	0.600	0.018	0.582
H_2O	1.200	0.800	0.400
CCl_4	0.00398	0.00025	0.00373
$K_2S_2O_8$	0.001	0.001	0
$NaHCO_3$	0.001	0.001	0
SLS	0.012	0.007	0.005

desired MWD. Figure 19 presents the evolution of the feed rates of styrene and CCl_4 used in this run. It can be seen that a constant feed rate was used during the first 16 min. Once the value of $\bar{n} \times N_p$ was estimated, the controller calculates higher feed rates to be added to the reactor. The CCl_4 was completely fed into the reactor after 36 min. From this moment, the polymerization was controlled by the feed rate of styrene. For this run the last half of the process was devoted to producing only 20% of the polymer, because at the end of the process a low concentration of styrene should be used to produce the low molecular-weight portion of the MWD.

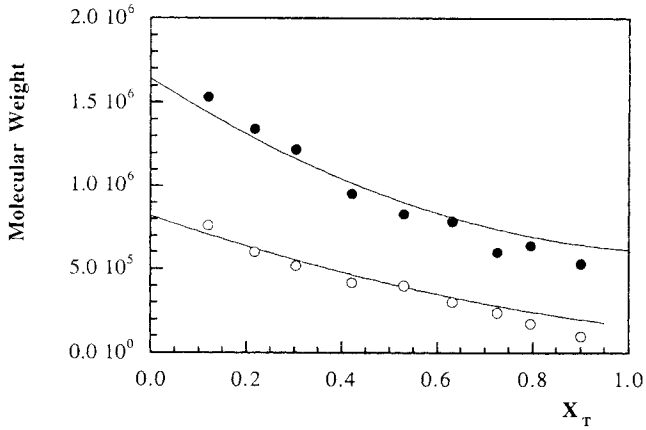

Figure 17. Evolution of $\bar{M}_w$ and $\bar{M}_n$ for case C2.

(—) desired; (●) experimental $\bar{M}_w$; (○) experimental $\bar{M}_n$.

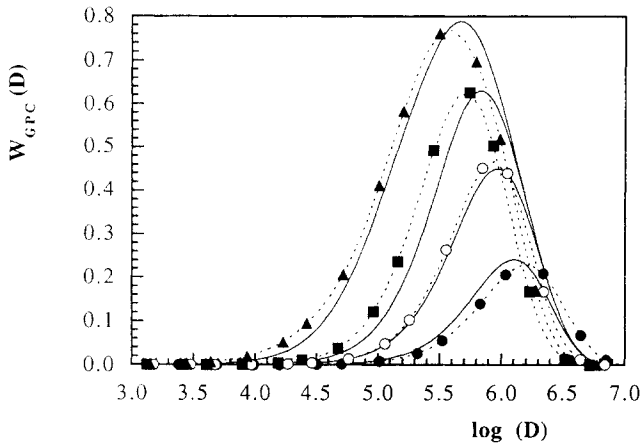

Figure 18. Evolution of the MWD for case C2.

(—) desired; experimental (--●--) $X_T = 0.20$, (--○--) $X_T = 0.42$, (--■--) $X_T = 0.62$ (--▲--) $X_T = 0.92$.

Case C3. The desired MWD was a bimodal distribution including two peaks, each of them of minimum polydispersity (PI = 2), plus the same amount of polymer. The optimal process is to produce the high molecular-weight peak during the first part of the polymerization (up to $X_T = 0.5$) by keeping the instantaneous MWD constant. The low molecular-weight peak is produced in a similar way during the second half of the process. Part of the CCl_4 is included in the initial charge, and up to $X_T = 0.5$ only styrene was fed into the reactor following the feed rates calculated by the nonlinear model-based controller (Figure 20). At $X_T = 0.5$ the rest of the CCl_4 was added to the reactor and again only the styrene feed rate was used to control the MWD. Figure 20 shows that the second part of the process lasted almost 7 h (as compared with 1.5 h needed for the first 50% of conversion). This was due to the small $[M]_p$ required to produce the low molecular-weight peak. Figures 21 and 22 present a comparison between the

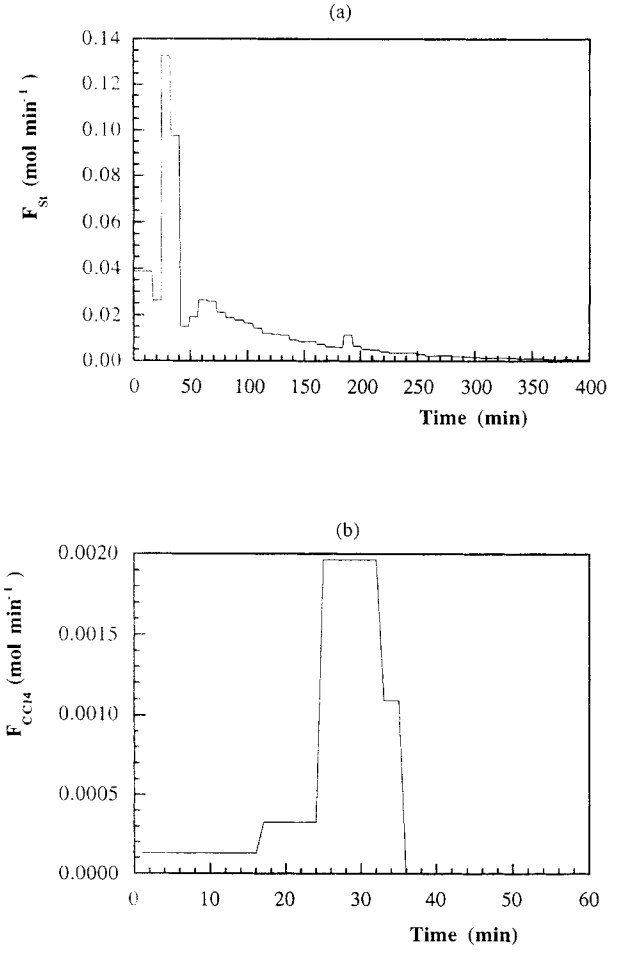

Figure 19. Feed-rate profiles calculated by the controller for case C2.

(a) styrene feed rate; (b) CCl_4 feed rate.

Table 6. Recipes Used in Case C3

Kg	Total	Initial Charge	Feed
St	0.600	0.042	0.558
H_2O	1.200	0.800	400
CCl_4	0.00643	0.000943	0.0055
$K_2S_2O_8$	0.001	0.001	0
$NaHCO_3$	0.001	0.001	0
SLS	0.012	0.007	0.005

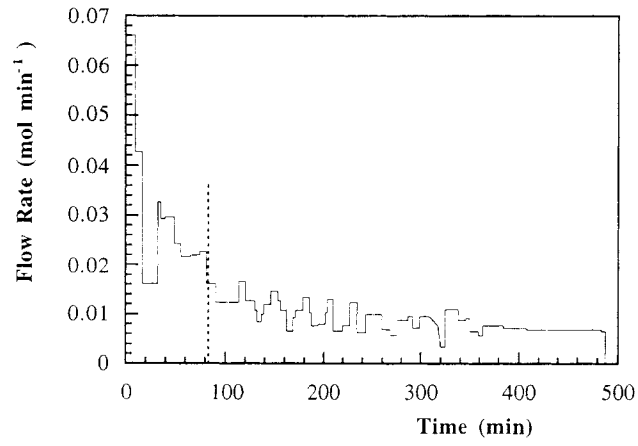

Figure 20. Styrene feed-rate profile for case C3.

(—) styrene feed rate; (--) second addition of CCl_4 ($X_T = 0.5$).

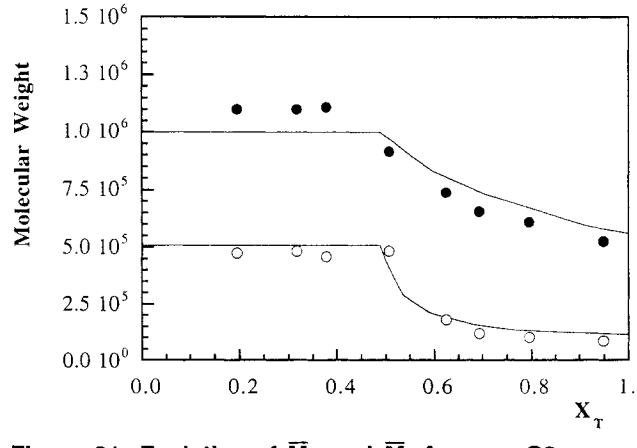

Figure 21. Evolution of $\overline{M}_w$ and $\overline{M}_n$ for case C3.

(—) desired; (●) experimental $\overline{M}_w$; (○) experimental $\overline{M}_n$.

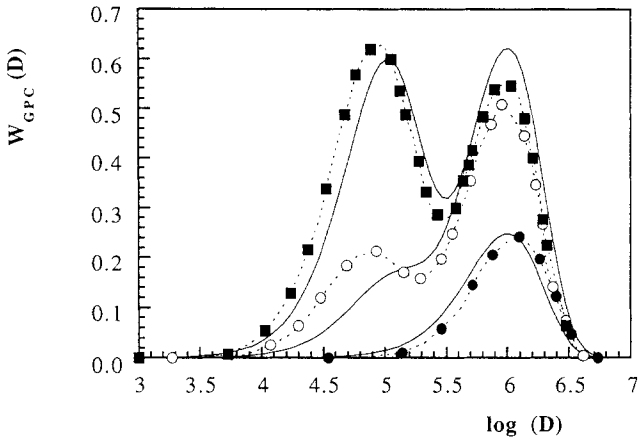

Figure 22. Evolution of the MWD for case C3.

(—) desired; experimental: (--●--) $X_T = 0.22$, (--○--) $X_T = 0.63$, (--■--) $X_T = 0.95$.

tween the desired $\overline{M}_w$, $\overline{M}_n$, and MWD and those obtained in the controlled process. It can be seen that the polymer obtained had the desired quality.

Conclusions

In this work, emulsion polymers with well-defined molecular-weight distributions were obtained by using a control strategy based on on-line GC measurements of the unreacted monomer and CTA. The measurements were filtered by means of a nonlinear optimization algorithm that minimizes the differences between the on-line measurements and the predictions of a mathematical model for the process. A nonlinear model-based controller was used to calculate the feed rates of monomer and CTA required to obtain the desired MWD in the shortest process time. This requires a mathematical model for the MWD that was developed based on independent measurements. The control strategy was first assessed by numerical simulation and then experimentally verified during the styrene emulsion polymerization using CCl_4 as CTA. Three different cases were considered: (C1) polymer of a given $\overline{M}_w$ and minimum polydispersity; (C2) polymer of arbitrary $\overline{M}_w$ and PI; and (C3) polymer with bimodal MWD. In all cases, the control strategy allowed us to produce the desired polymer quality.

Acknowledgments

The financial support from the Diputación Foral de Gipuzkoa and the CICYT (grant MAT94-002) is gratefully appreciated. A. Echevarría acknowledges the fellowship from the Basque Government.

Literature Cited

Adebekun, D. K., and F. J. Schork, "Continuous Solution Polymerization Reactor Control. 2. Estimation and Nonlinear Reference Control during Methyl Methacrylate Polymerization," *Ind. Eng. Chem. Res.*, **28**, 1846 (1989).

Armitage, P. D., J. C. de la Cal, and J. M. Asua, "Improved Methods for Solving Monomer Partitioning in Emulsion Copolymer Systems," *J. Appl. Poly. Sci.*, **51**, 1985 (1994).

Baus, R. E., and G. Swift, U.S. Patent No. 4,501,845 (1985).

Billmeyer, F. W., *Textbook of Polymer Science*, Wiley-Interscience, New York (1962).

Brandup, J., and E. H. Immergut, eds., *Polymer Handbook*, 2nd ed., Wiley-Interscience, New York (1989).

Buback, M., L. M. García-Rubio, R. G. Gilbert, D. H. Napper, J. Guillot, A. E. Hamielec, D. Hill, K. F. O'Driscoll, F. J. Olag, J. Shen, D. Solomon, G. Moad, M. Stickler, M. Tirrell, and M. A. Winnick, "Consistent Values of Rate Parameters in Free Radical Polymerization Systems," *J. Poly. Sci., Poly. Lett. Ed.*, **26**, 293 (1988).

Budde, U., and K. M. Reichert, "Automatic Polymerization Reactor with On-Line Data Measurement and Reactor Control," *Angew. Makromol. Chem.*, **161**, 195 (1988).

Canu, P., S. Canegallo, S. Morbidelli, and G. Storti, "Polymer Quality Control in Latex Semibatch Reactors Through On-line Monitoring of Conversion," *J. Apply. Poly. Sci.*, **54**, 1998 (1994).

Echevarría, A., J. C. de la Cal, and J. M. Asua, "Minimum-Time Strategy to Produce Nonuniform Emulsion Copolymers: I. Theory," *J. Appl. Poly. Sci.*, **57**, 1063 (1995).

Ellis, M. F., T. W. Taylor, V. González, and K. F. Jensen, "Estimation of the Molecular Weight Distribution in Batch Polymerization," *AIChE J.*, **34**, 1341 (1988).

Ellis, M. F., T. W. Taylor, V. González, and K. F. Jensen, "On-line Molecular Weight Distribution Estimation and Control in Batch Polymerization," *AIChE J.*, **40**, 445 (1994).

Gardon, J. L., "Emulsion Polymerization. VI. Concentration of Monomers in Polymer Particles," *J. Poly. Sci., Part A-1*, **6**, 2859 (1968).

Gugliotta, L. M., G. Arzamendi, and J. M. Asua, "Choice of the Monomer Partition Model in Mathematical Modeling of Emulsion Copolymerization System," *J. Appl. Poly. Sci.*, **55**, 1231 (1995).

Jang, S. S., B. Joseph, and H. Munai, "Comparison of Two Approaches to On-Line Parameter and State Estimation of Non-Linear Systems," *Ind. Eng. Chem. Process Des. Dev.*, **25**, 809 (1986).

Jo, J. M., and S. O. Bankoff, "Real Time Estimation of Polymerization Reactors," *AIChE J.*, **22**, 361 (1976).

Leiza, J. R., J. C. de la Cal, M. Montes, and J. M. Asua, "On-Line Monitoring of Conversion and Polymer Composition in Emulsion Polymerization Systems," *Proc. Control Qual.*, **4**, 197 (1993).

Nelder, J. A., and R. Mead, "A Simplex Method for Function Minimization," *Comput. J.*, **7**, 308 (1965).

Ponnusvamy, S., L. L. Shah, and C. Kiparissides, "On-Line Monitoring of Polymer Quality in a Batch Polymerization Reactor," *J. Appl. Poly. Sci.*, **32**, 3239 (1988).

Schuler, H., and S. Suzhen, "Real Time Estimation of the Chain Length Distribution in a Polymerization Reactor," *Chem. Eng. Sci.*, **40**, 1891 (1985).

Schuler, H., and S. Papadopoulou, "Real Time Estimation of the Chain Length Distribution in a Polymerization Reactor: II. Comparison of Estimated and Measured Distribution Functions," *Chem. Eng. Sci.*, **41**, 2681 (1986).

Seinfeld, J. H., and L. Lapidus, *Mathematical Methods in Chemical Engineering*, Vol. 3, *Process Modeling, Estimation and Identification*, Prentice Hall, Englewood Cliffs, NJ (1974).

Urretabizkaia, A., J. R. Leiza, and J. M. Asua, "On-Line Terpolymer Composition Control in Semicontinuous Emulsion Polymerization," *AIChE J.*, **40**, 1850 (1994).

Appendix A: Experimental Details

Styrene (St) was distilled under reduced pressure of dry nitrogen and stored at −18°C until use. Sodium lauryl sulfate (SLS, Merck), potassium persulfate (Fluka), and sodium bicarbonate (Panreac) were used as received. Deionized water was used throughout the work. Polymerizations were carried out at 60°C in a 2-L stainless-steel reactor equipped with stirrer, sampling device, and inlet system for nitrogen. In the batch polymerizations, samples were withdrawn during the reaction, the polymerization short stopped with hydroquinone, the monomer conversion determined by gravimetry, and the CCl_4 conversion measured by gas chromatography (GC, Shimazdu, GC 14-A). The particle size was measured by dynamic light scattering (COULTER N4-PLUS). The

number of polymer particles was estimated from the values of conversion and particle size. The MWD was measured by GPC using two columns (Styragel HR6 and Styragel HR4, Waters) and a refractive index detector.

Appendix B: Discretization of the MWD

In order to calculate the instantaneous MWD that has to be produced at each value of X_T, the final MWD is discretized as follows:

$$W_c^*(n) = \frac{1}{X_{Tf}} \sum_{j=1}^{k} W_j(n) \Delta X_{Tj} = \frac{\Delta X_T}{X_{Tf}} \sum_{j=1}^{k} \frac{n}{\bar{X}_{ni_j}^2} \exp\left(-\frac{n}{\bar{X}_{ni_j}}\right), \quad \text{(B1)}$$

where X_{Tf} is the final overall conversion, $W_j(n)$ is the instantaneous distribution produced in the conversion increment (a constant value of ΔX_{Tj} (ΔX_T) is used in Eq. B1), and k is the number of increments into which X_{Tf} is divided. For a given number of conversion increments, the required values of $\bar{X}_{ni_j}$ can be calculated by minimizing the following equation:

$$\underset{\bar{X}_{ni}}{\text{Min}} \left[\sum_n \left(W_c^d(n) - W_c^*(n)\right)^2 \right], \quad \text{(B2)}$$

where $W_c^d(n)$ and $W_c^*(n)$ are the desired and the calculated MWDs. The number of values of n should be greater than the number of conversion increments. Typically, 100 values of n were used for $k = 20$. It is worth pointing out that the larger the number of conversion increments, the closer to the desired MWD will be the solution, but the computation time will increase as the number of parameters to be estimated, $\bar{X}_{ni}$, increases.

The minimization of Eq. B2 gives the values of $\bar{X}_{ni}$ to be produced at different ΔX_T, but it does not provide any hint about the sequence in which they have to be produced. This sequence can be inferred by assuming that the CCl_4 is much less reactive than styrene and accumulates in the reactor, precluding the formation of high molecular-weight polymer at the end of the process. Therefore, the best sequence is to produce a continuously decreasing molecular-weight polymer during the process (an exception to this rule is the production of an MWD of minimum polydispersity index when the same molecular weight has to be produced throughout the process).

Manuscript received Oct. 9, 1997, and revision received Apr. 20, 1998.